Contribution of diffusion-weighted MRI to the differential diagnosis of hepatic masses

Özgün İlhan Demir, Funda Obuz, Özgül Sağol, Oğuz Dicle

PURPOSE
To evaluate the diagnostic contribution of diffusion-weighted magnetic resonance imaging (MRI) using apparent diffusion coefficient (ADC) values to the characterization of hepatic masses and differentiation of benign and malignant lesions.

MATERIALS AND METHODS
The study included 30 patients that underwent upper abdominal MRI examinations because of hepatic masses that were found to be ≥1 cm in size with conventional sequences, and were additionally evaluated with diffusion-weighted MRI. Diffusion-weighted images and ADC maps in the axial plane were obtained using a 1.5 Tesla MRI device, single shot echo-planar spin echo sequences on 3 axes (x, y, z), and diffusion sensitive gradients with 2 different b values (b = 0 and b = 1000 s/mm^2). Mean ADC measurements were calculated among the 30 cases involving 41 hepatic masses.

RESULTS
Of the 41 hepatic masses, 24 were benign and 17 were malignant. Benign lesions included 6 cysts, 14 hemangiomas, 2 abscesses, and 2 hydatid cysts. Malignant masses included 8 metastases, 4 hepatocellular carcinomas, 4 cholangiocellular carcinomas, and 1 gall bladder adenocarcinoma. The highest ADC values were for cysts and hemangiomas. The mean ADC value of benign lesions was $2.57 \pm 0.26 \times 10^{-3}$ mm^2/s, whereas malignant lesions had a mean ADC value of $0.86 \pm 0.11 \times 10^{-3}$ mm^2/s. The mean ADC value of benign lesions was significantly higher than that of malignant lesions ($P < 0.01$).

CONCLUSION
Diffusion-weighted MRI with quantitative ADC measurements can be useful in the differentiation of benign and malignant liver lesions.

Key words: • liver • magnetic resonance imaging • diffusion

From the Departments of Radiology (Ö.İ.D., F.O. ✉ *fobuz@deu. edu.tr*, O.D.), and Pathology (Ö.S.), Dokuz Eylül University School of Medicine, İzmir, Turkey.

The liver is an organ in which various benign or malignant primary or secondary masses can be detected. Today, focal masses are diagnosed using ultrasonography (US) and/or computed tomography (CT). Additionally, magnetic resonance imaging (MRI) is preferred when further characterization of these masses is needed. MRI has many advantages (e.g., high contrast resolution, the ability to obtain images in any plane, lack of ionizing radiation, and the safety of using particulate contrast media rather than those containing iodine) that make it a favored modality. Lesion morphology, signal intensity, and contrast enhancement pattern are taken into consideration when characterizing masses with MRI; however, even if the data are evaluated together, there can still be difficulties in the differentiation of benign and malignant lesions. Although dynamic contrast enhanced examinations have become a routine component of abdominal imaging, the high cost/benefit ratio and risk of contrast media side effects remain an issue. Moreover, sometimes it is not possible to distinguish between highly vascular metastases and hemangiomas, even using dynamic examinations (1). In hepatic MRI, artifacts due to cardiac activity, respiration, and intestinal peristalsis can negatively affect imaging quality, especially in T2-weighted sequences, which require a relatively long time to acquire, particularly in elderly patients.

Diffusion-weighted MRI, first used for the early diagnosis of stroke in neuroradiology, is a technique that acquires an image during a single breath-hold and does not require contrast medium (2–4). In the past, this technique was limited to cranial examinations because of its sensitivity to cardiac, respiratory, and peristaltic movements; however its usage has spread among other body parts after the development of fast MRI sequences, like eco-planar imaging (EPI). Muller et al. first reported in 1994 on diffusion-weighted MRI of normal hepatic, splenic, and muscular tissues, as well as on focal and diffuse hepatic diseases, and obtained significant results (5). In the years that followed, several studies on liver, kidney, and other abdominal organs examined with diffusion-weighted MRI were published (6–13). In these studies it was shown that apparent diffusion coefficient (ADC) values of normal tissues and lesions can be measured using diffusion-weighted images, and the differences in ADC values can be used in the differential diagnosis.

The major aim of the present study was to measure the ADC values of benign and malignant focal mass lesions of the liver using diffusion-weighted MRI and to determine their contribution to differential diagnosis.

Materials and methods

The study included conscious adult patient volunteers over 18 years of age with primary or metastatic hepatic tumors, or non-tumoral masses

that were determined by US or CT between November 2003 and June 2005. Patients with a poor general condition, who were unable to maintain a breath-hold, or had a contraindication for MRI (i.e., MRI incompatible prosthesis and cardiac pace-maker holders) were excluded from the study. The study protocol was approved by the ethical committee of our university and all the patients gave informed consent. Patients were between 18 and 88 years old (mean age, 54.4 years). In all, 30 patients (15 males and 15 females) with a total of 41 hepatic masses participated in the study.

Simple hepatic cysts (n = 6) were diagnosed with typical US and MRI findings. Hemangiomas (n = 14) were diagnosed easily with their characteristic MRI findings and typical contrast enhancement patterns. Histopathological evaluations were performed to diagnose pyogenic and amoebic abscesses following surgery. One hydatid cyst was diagnosed histopathologically and the other one based on serologic and radiological features. Of the 8 metastatic masses, 5 were encountered in patients with known primary malignancy (2 breast cancers, 1 lung cancer, 1 renal cell carcinoma, 1 Hodgkin's lymphoma) and with diagnosed metastasis, as they were discovered during routine screening and they tended to increase in size with time. The 3 remaining metastatic liver masses were evaluated with biopsy and diagnosed as metastatic adenocarcinoma of unknown origin. One of the cases was diagnosed with imaging techniques (CT and MRI) and appeared to be a gall bladder tumor with local hepatic invasion. Of the 4 lesions of primary hepatocellular tumors of the liver, one was a hepatoblastoma, diagnosed histopathologically. The 3 remaining lesions were hepatocellular carcinoma (HCC) cases with portal vein thrombosis, of which 2 were

diagnosed histopathologically, and one with MRI. Among the 4 cases of cholangiocellular carcinoma, 2 were diagnosed histopathologically and the others with MRI. The 41 masses ranged in diameter from 1 to 17 cm (mean diameter, 7.4 cm) (Table 1).

Routine upper abdominal MRI examinations were performed in the 30 patients using a 1.5 Tesla MRI device (Gyroscan Intera, Philips, ACS-NT, Best, The Netherlands) and a phased array coil. Routine examinations were composed of the following sequences: fat suppressed TSE T2-weighted (TR/TE, 1600/70 ms; flip angle, 90°; slice thickness, 5 mm; FOV, 375 mm); TSE heavily T2-weighted (TR/TE, 1320/325 ms); gradient echo in-phase and opposed-phase T1-weighted (TR/TE, 192/5 ms [in-phase], 250/7 ms [opposed-phase]; flip angle, 80°); contrast enhanced dynamic T1-weighted images (TR/TE, 176/7 ms; flip angle, 70°) in the axial plane. Diffusion-weighted MRI examinations were performed before contrast enhanced slices were obtained. Diffusion-weighted sequences (TR/TE, 4200/95 ms; flip angle, 90°; slice thickness, 5 mm; FOV, 230–340; breath-holding time, 50 s) in the axial plane were performed, applying gradients (in order to sensitize SE sequence to diffusion) to single-shot echo-planar sequences in all 3 axes (x, y, z), and 2 different b values (b = 0 s/mm^2 and b = 1000 s/mm^2). The first series of the image set was composed of echo-planar spin echo T2-weighted images (b = 0 s/mm^2), the next 3 series of images were applied to the first series in x, y, and z axes (value of diffusion sensitive gradients, b = 1000 s/mm^2), and the

last series of isotropic images were calculated from the projection of the diffusion vectors in all 3 axes. Isotropic images consisted of images that were calculated by obtaining the cube root of multiplication of signal intensities that were measured by the device in x, y, and z axes, and images that removed axes-dependent signal differences. ADC maps regarding isotropic images were formed automatically by the device and all mean ADC values of the lesions were measured on those maps.

A circular region of interest (ROI) 1 cm in diameter was used in order to measure the lesions. In large lesions the mean value of 3 different ROI measurements on the same slice was calculated. Again, for every lesion, a mean ADC value was determined by taking the mean of ADC measurements of successive slices. For heterogeneous lesions, measurements were performed from contrast enhanced solid parts on conventional sequences and post-contrast images. The ADC value of lesions 1 cm in diameter was established using a single ROI. Statistical analyses were performed using the Mann-Whitney U test in a computer software (SPSS Inc., Chicago, Illinois, USA).

Results

The mean ADC value of the 24 benign lesions was $2.57 \pm 0.26 \times 10^{-3}$ mm^2/s. ADC values of benign lesions were between $1.09 \pm 0.32 \times 10^{-3}$ and $3.36 \pm 0.28 \times 10^{-3}$ mm^2/s (Table 2). The highest ADC value was for simple cysts (Fig. 1). Among the benign lesions, pyogenic abscesses had the lowest ADC value (Fig. 2).

Table 1. Distribution of lesions according to size

Size of lesions	Number of lesions
1 cm	3
1–5 cm	13
5–10 cm	13
>10 cm	12

Table 2. Mean apparent diffusion coefficient (ADC) values according to lesion type

Lesion type	Mean ADC (mm²/s)
Simple cyst	$3.05 \pm 0.26 \times 10^{-3}$
Hemangioma	$2.46 \pm 0.21 \times 10^{-3}$
Hydatid cyst	$2.99 \pm 0.24 \times 10^{-3}$
Pyogenic abscess	$1.09 \pm 0.32 \times 10^{-3}$
Amoebic abscess	$1.83 \pm 0.28 \times 10^{-3}$
Metastasis	$0.79 \pm 0.11 \times 10^{-3}$
Hepatocellular carcinoma	$0.90 \pm 0.10 \times 10^{-3}$
Cholangiocellular carcinoma	$0.95 \pm 0.13 \times 10^{-3}$
Gall bladder tumor	$0.87 \pm 0.10 \times 10^{-3}$

Figure 1. a–c. A 59-year-old female patient with a simple hepatic cyst. On axial fat suppressed T2-weighted MR image **(a)**, a hyperintense lesion consistent with a simple cyst in the right lobe of the liver is seen. On diffusion-weighted MR image **(b)**, the lesion is isointense compared to the liver. Hyperintensity on the ADC map **(c)** regarding apparent diffusion increase (mean ADC, $3.24 \pm 0.21 \times 10^{-3}$).
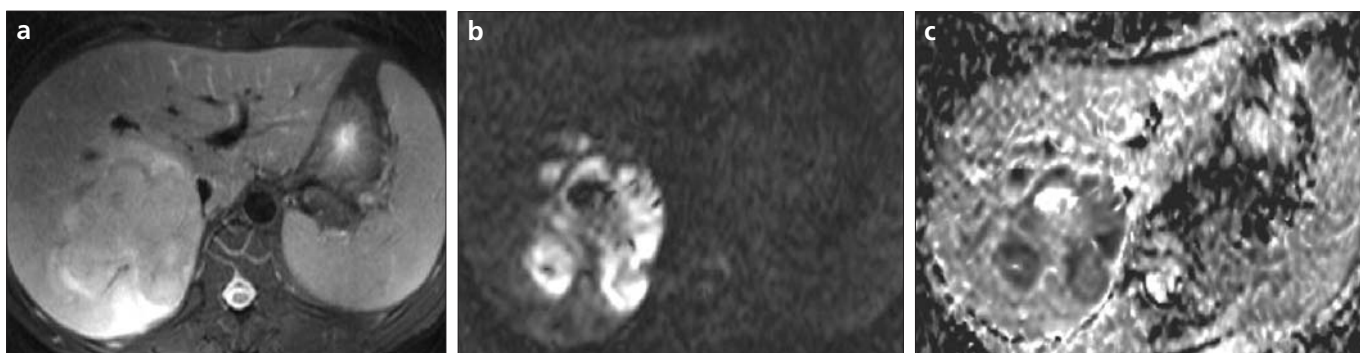

Figure 2. a–c. A 50-year-old male patient with a pyogenic hepatic abscess. On axial fat suppressed T2-weighted MR image **(a)**, a hyperintense lesion in right lobe is seen. Increase in intensity due to diffusion restriction on diffusion-weighted MRI **(b)**. Increase in intensity confirming diffusion restriction on ADC map **(c)** (mean ADC, $1.09 \pm 0.32 \times 10^{-3}$).

The ADC values of the 17 malignant lesions were between 0.54 ± 0.07 and $1.24 \pm 0.14 \times 10^{-3}$ mm^2/s, with a mean value of $0.86 \pm 0.11 \times 10^{-3}$ mm^2/s (Table 2, Fig. 3). Among the malignant lesions, the lowest ADC value was for breast cancer metastasis, while cholangiocellular carcinoma had the highest value (Fig. 4). The difference between the mean ADC values of benign and malignant lesions was statistically significant ($P < 0.01$).

Discussion

Diffusion is the term used for the randomized microscopic movement of water molecules. Diffusion is known to be a sensitive parameter in microscopic tissue characterization. Currently, it is possible to determine diffusion by measuring diffusion-weighted MRI and ADC in vivo (14). Diffusion-weighted imaging can be performed after strong bipolar pulses are added to spin echo or gradient echo sequences, by sensitizing the water in tissue to diffusion. Thus, the mobility and viscosity of water molecules can be evaluated, and water balance between intracellular and extracellular compartments can be seen (15).

Diffusion-weighted MRI examinations have many technical restrictions, such as respiratory, cardiac, or peristaltic physiologic activity, all of which affect image quality and make evaluation, which is very sensitive to motion, more difficult. Consequently, prior to the development of fast MRI techniques, diffusion-weighted imaging was limited to cranial examinations. With the development of echo-planar imaging, a fast MRI technique, radiologists have overcome the long imaging times and related artifacts of conventional techniques, and diffusion-weighted MRI is now available for abdominal evaluations as well (5, 16).

The amount of diffusion is defined using the diffusion coefficient. Diffusion coefficient measurement in vivo is affected by several factors in biological tissues. Capillary perfusion, temperature, magnetic sensitivity of the tissue, and motion affects the actual diffusion; therefore, the term "apparent diffusion coefficient" (ADC) is used rather than "diffusion coefficient" (17).

The following formula is used to calculate ADC:

$$SI/SI_0 = \exp(-b \times ADC) \quad (18)$$

where SI indicates the signal intensity of the diffusion gradient (b) applied to the image, SI_0 is the signal intensity prior to the gradient application and b is the value of the applied diffusion gradient.

The formula can be applied as follows, when there are 2 different b values:

$$ADC = [\ln(S1/S2)] /(b2-b1) \quad (19)$$

In order to calculate the diffusion gradient (b), the following formula is used which includes the gradient application time (λ), power of the gradient (G), time between gradients (Δ), and gyromagnetic ratio (γ):

$$b = \gamma^2 \, G^2 \, \lambda^2 \, (\Delta - \lambda/3)$$

In the present study, ADC measurements of benign and malignant hepatic masses were significantly different, which supports similar previous findings (8, 19–21). Cysts and hemangiomas had the highest ADC values,
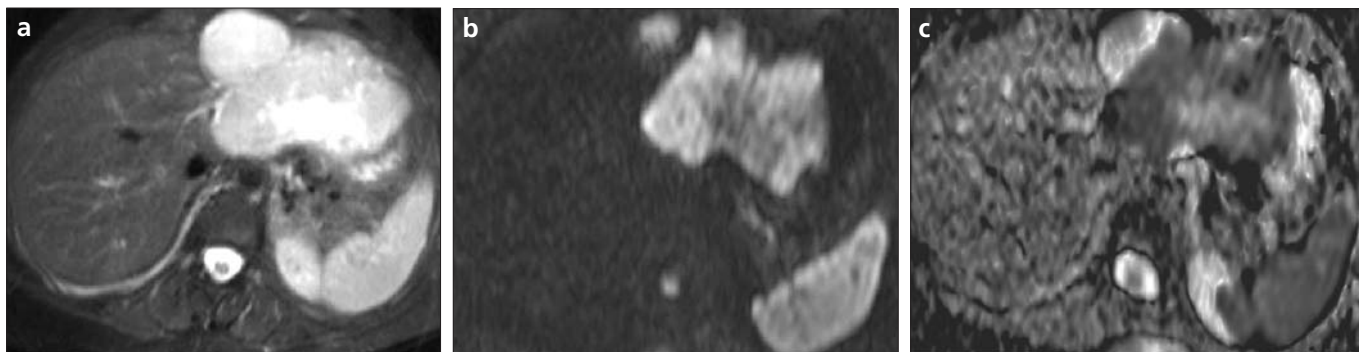
Figure 3. a–c. A 47-year-old female patient with metastatic lung cancer. On axial fat suppressed T2-weighted MR image **(a)**, a hyperintense mass lesion with necrosis in the center is seen. Diffusion-weighted MR image **(b)** shows increased intensity due to diffusion restriction. The lesion is observed as hypointense on ADC map **(c)** (mean ADC, $0.76 \pm 0.08 \times 10^{-3}$).

Figure 4. a–c. A 62-year-old male patient with cholangiocellular carcinoma. A hyperintense lesion with a slightly heterogeneous inner structure, particularly in the right lobe, and extending to segment 4a–b is seen on fat suppressed T2-weighted MR image **(a)**. Increase in intensity due to diffusion restriction on diffusion-weighted MRI **(b)**. Increase in intensity confirming diffusion restriction on ADC map **(c)** (mean ADC, $0.83 \pm 0.12 \times 10^{-3}$).

while malignant masses had the lowest. The mean ADC value for cystic lesions was $3.05 \pm 0.26 \times 10^{-3}$ s/mm^2, whereas for hemangiomas it was $2.46 \pm 0.21 \times 10^{-3}$ s/mm^2. Overlapping values were present among these 2 groups. Two hemangiomas in our study had ADC values $>3.00 \times 10^{-3}$ s/mm^2 (3.28 ± 0.19 and $3.07 \pm 0.17 \times 10^{-3}$ s/mm^2). All the simple cystic lesions had higher ADC values than mean ADC value of hemangiomas (Fig. 1).

The lowest ADC values among the malignant masses belonged to metastases (Fig. 3). This data is similar to Taouli et al.'s findings (20). Mean ADC value for HCC was $0.90 \pm 0.10 \times 10^{-3}$ s/mm^2 and for cholangiocellular carcinoma it was $0.95 \pm 0.13 \times 10^{-3}$ s/mm^2 (Fig. 4). Mean ADC value for all malignant masses was $0.86 \pm 0.11 \times 10^{-3}$ s/mm^2.

The mean ADC value for the pyogenic abscess was $1.09 \pm 0.32 \times 10^{-3}$ s/mm^2 (Fig. 2). This low value could be related to the dense viscous content of the abscess. According to a study by Chan et al. on the use of MRI for the differentiation of abscesses and necrotic tumors (22), the mean ADC value was significantly lower for hepatic abscesses compared to necrotic tumors and simple cysts ($0.67 \pm 0.35 \times 10^{-3}$ s/mm^2). There were no necrotic or cystic lesions among the malignant tumors in our study. Thus, the pyogenic abscess had a significantly lower ADC value compared to simple cysts.

The mean ADC value was $1.83 \pm 0.28 \times 10^{-3}$ s/mm^2 in our case of an amoebic abscess. Different cavity content and viscosity could have been the reason why it was higher than the pyogenic abscess.

The mean ADC values of the 2 hydatid cysts were 3.03 ± 0.22 and $2.95 \pm 0.26 \times 10^{-3}$ s/mm^2. Unexpectedly, those values did not reflect an increase in viscosity related to cyst contents, and were not significantly different from simple cysts. To the best of our knowledge, there are no diffusion MRI studies dealing with hydatid cysts in the literature. With studies including larger series, we think that important data will be added to the literature on the use of diffusion-weighted MRI for the differential diagnosis of hydatid cysts and simple cysts.

As reported by Le Bihan et al., when the b value is lowered, the diffusion weight of the sequence becomes lower, signal loss according to diffusion decreases, and ADC value increases (23). In a study by Ichikawa et al., b values were quite low (i.e., 1.6, 16, and 55) and ADC values for abdominal organs were high (19). They reported that when the b value is kept low, factors like perfusion and T2 time have greater relative affect on ADC measurements. For that reason, they concluded that for abdominal diffusion studies, values >400 s/mm^2 might reflect ADC measurements more accurately (19). Our study was carried out with b values of 0 and 1000 s/mm^2; however, again, Ichikawa et al. reported that higher b values cause lower quality on diffusion-weighted images and make evaluation harder (19). In our study, adequate image quality could not be obtained with diffusion-weighted images because of high b values; however, that was not considered problematic since ADC

map measurements were taken into account.

Namimoto et al. (8) used 2 different b values (b = 30 and b = 1200 s/mm^2) in their study and on low b-value diffusion-weighted MR images (in low diffusion weighting) all masses were observed as hyperintense, whereas on high b-value images (in high diffusion weighting) signals of cysts disappeared and signals of hemangiomas obviously decreased. In contrast, since there is a limitation of diffusion in solid tumors, they were also observed as hyperintense on high b-value diffusion-weighted images.

In a study by Yamada et al. (24), actual diffusion coefficients (D) and ADC values of hepatic lesions were measured, and D values were lower than ADC values. They concluded that in vivo capillary perfusion affected the signals of diffusion-weighted images. Only in cystic lesions that did not have vascularity, ADC and D values were equal. Yamada et al. used following formula in order to calculate the D coefficient:

$$SI/SIo = (1-f) \times exp (-b.D) + f \times exp (-b.D^*)$$

where D and D* represent actual and fake diffusion coefficients, respectively, and f indicates perfusion fraction (23). According to this formula and the study, f and D coefficients may be useful for the characterization of hepatic lesions (23).

In the present study, measurement of actual diffusion was not our aim, because perfusion, temperature alterations, magnetic sensitivity, and motion affect diffusion measurements in biological tissues. Therefore, ADC measurements, with the contribution of these factors, provided significant results in lesion characterization.

We used 2 different b values in 3 axes (x, y, z) to achieve diffusion-weighted MR images. ADC maps were formed and ADC measurements were made using isotropic images. Taouli et al. reported that there was no difference between measured ADC values of normal and cirrhotic liver parenchyma, and focal hepatic lesions in 3 axes (20). Considering this data, it has been reported that liver parenchyma and focal liver lesions, contrary to cerebral white matter and kidneys, have an isotropic diffusion pattern, thus it is needless to use multi-dimensional diffusion gradients in liver diffusion studies (20).

One major limitation of our study, was the low number of lesions and the absence of benign hepatocellular lesions (e.g., hepatic adenoma, focal nodular hyperplasia), when subgroups are taken into consideration. Hence, comparison between solid benign and malignant masses or between different malignant masses could not be made. Benign hepatocellular mass lesions were first evaluated by Taouli et al. and their ADC values were found to be lower than cysts and hemangiomas, and higher than malignant masses (20).

Another limitation of our study was the extremely low spatial resolution due to high b value selection, especially in lesions <1 cm in diameter, and exclusion of those cases. In recent studies, image quality has been improved with faster parallel imaging methods (e.g., sensitivity encoding = SENSE) and so EPI-related artifacts have been reduced (25–27). Additionally, there are publications that report improved image quality in diffusion MRI studies with 3 Tesla MRI devices (28). The latest improvements to fusion software make it possible to superimpose diffusion-weighted MRI images onto routine MRI images, automatically or manually, overcoming difficulties in the localization of lesions.

In conclusion, the diffusion-weighted MRI sequence is a useful diagnostic tool since it can be obtained during a single breath-hold, there is no need to use contrast media, and it can contribute to accurate diagnosis when discrimination of benign and malignant hepatic masses cannot be accomplished by conventional MRI sequences.

References

1. Semelka RC, Shoenut JP, Kroeker MA, et al. Focal liver disease: comparison of dynamic contrast-enhanced CT and T2-weighted fat-suppressed, FLASH, and dynamic gadolinium-enhanced MR imaging at 1.5 T. Radiology 1992; 184:687–694.
2. Warach S, Chien D, Li W, Ronthal M, Edelman RR. Fast magnetic resonance diffusion-weighted imaging of acute human stroke. Neurology 1992; 42:1717–1723.
3. Back T, Hoehn-Berlage M, Kohno K, Hossmann KA. Diffusion nuclear magnetic resonance imaging in experimental stroke: correlation with cerebral metabolites. Stroke 1994; 25:494–500.
4. Lutsep HL, Albers GW, DeCrespigny A, Kamat GN, Marks MP, Moseley ME. Clinical utility of diffusion-weighted magnetic resonance imaging in the assessment of ischemic stroke. Ann Neurol 1997; 41:574–580.
5. Muller MF, Prasad P, Siewert B, Nissenbaum MA, Raptopoulos V, Edelman RR. Abdominal diffusion mapping with use of a whole-body echo-planar system. Radiology 1994; 190:475–483.
6. Kim T, Murakami T, Takahashi S, Hori M, Tsuda K, Nakamura H. Diffusion-weighted single-shot echoplanar MR imaging for liver disease. AJR Am J Roentgenol 1999; 173:393–398.
7. Ichikawa T, Haradome H, Hachiya J, Nitatori T, Araki T. Diffusion-weighted MR imaging with a single-shot echoplanar sequence: detection and characterization of focal hepatic lesions. AJR Am J Roentgenol 1998; 170:397–402.
8. Namimoto T, Yamashita Y, Sumi S, Tang Y, Takahashi M. Focal liver masses: characterization with diffusion-weighted echo-planar MR imaging. Radiology 1997; 204:739–744.
9. Stahlberg F, Brockstedt S, Thomsen C, Wirestam R. Single-shot diffusion-weighted echo-planar imaging of normal and cirrhotic livers using a phased-array multicoil. Acta Radiol 1999; 40:339.
10. Amano Y, Kumazaki T, Ishihara M. Single-shot diffusion-weighted echo-planar imaging of normal and cirrhotic livers using a phased-array multicoil. Acta Radiol 1998; 39:440–442.
11. Moteki T, Ishizaka H, Horikoshi H, Matsumoto M. Differentiation between hemangiomas and hepatocellular carcinomas with the apparent diffusion coefficient calculated from turboFLASH MR images. J Magn Reson Imaging 1995; 5: 187–191.
12. Ries M, Jones RA, Basseau F, Moonen CT, Grenier N. Diffusion tensor MRI of the human kidney. J Magn Reson Imaging 2001; 14:42–49.
13. Namimoto T, Yamashita Y, Mitsuzaki K, Nakayama Y, Tang Y, Takahashi M. Measurement of the apparent diffusion coefficient in diffuse renal disease by diffusion-weighted echo-planar MR imaging. J Magn Reson Imaging 1999; 9:832–837.
14. Le Bihan D, Turner R, Douek P, Patronas N. Diffusion MR imaging: clinical applications. AJR Am J Roentgenol 1992; 159: 591–599.
15. Hagmann P, Jonasson L, Maeder P, Thiran JP, Wedeen VJ, Meuli R. Understanding diffusion MR imaging techniques: from scalar diffusion-weighted imaging to diffusion tensor imaging and beyond. Radiographics 2006; 26:205–223.
16. Reimer P, Saini S, Hahn PF, Brady TJ, Cohen MS. Clinical application of abdominal echoplanar imaging (EPI): optimization using a retrofitted EPI system. J Comput Assist Tomogr 1994; 18:673–679.
17. Le Bihan D. Molecular diffusion nuclear magnetic resonance imaging. Magn Reson Q 1991; 7:1–30.
18. Le Bihan D, Breton E, Lallemand D, Grenier P, Cabanis E, Laval-Jeantet M. MR imaging of intravoxel incoherent motions: application to diffusion and perfusion in neurologic disorders. Radiology 1986; 161:401–407.
19. Ichikawa T, Haradome H, Hachiya J, Nitatori T, Araki T. Diffusion-weighted MR imaging with single-shot echo-planar imaging in the upper abdomen: preliminary clinical experience in 61 patients. Abdom Imaging 1999; 24:456–461.

20. Taouli B, Vilgrain V, Dumont E, Daire JL, Fan B, Menu Y. Evaluation of liver diffusion isotropy and characterization of focal hepatic lesions with two single-shot echo-planar MR imaging sequences: prospective study in 66 patients. Radiology 2003; 226:71–78.
21. Moteki T, Horikoshi H, Oya N, Aoki J, Endo K. Evaluation of hepatic lesions and hepatic parenchyma using diffusion-weighted reordered turboFLASH magnetic resonance images. J Magn Reson Imaging 2002; 15:564–572.
22. Chan JH, Tsui EY, Luk SH, et al. Diffusion-weighted MR imaging of the liver: distinguishing hepatic abscess from cystic or necrotic tumor. Abdom Imaging 2001; 26: 161–165.
23. Le Bihan D, Breton E, Lallemand D, Aubin ML, Vignaud J, Laval-Jeantet M. Separation of diffusion and perfusion in intravoxel incoherent motion MR imaging. Radiology 1988; 168:497–505.
24. Yamada I, Aung W, Himeno Y, Nakagawa T, Shibuya H. Diffusion coefficients in abdominal organs and hepatic lesions: evaluation with intravoxel incoherent motion echo-planar MR imaging. Radiology 1999; 210:617–623.
25. Bammer R, Keeling SL, Augustin M, et al. Improved diffusion-weighted single-shot echo-planar imaging (EPI) in stroke using sensitivity encoding (SENSE). Magn Reson Med 2001; 46:548–554.
26. Nasu K, Kuroki Y, Nawano S, et al. Hepatic metastases: diffusion-weighted sensitivity-encoding versus SPIO-enhanced MR imaging. Radiology 2006; 239:122–130.
27. Yoshikawa T, Kawamitsu H, Mitchell DG, et al. ADC measurement of abdominal organs and lesions using parallel imaging technique. AJR Am J Roentgenol 2006; 187:1521–1530.
28. Hunsche S, Moseley ME, Stoeter P, Hedehus M. Diffusion-tensor MR imaging at 1.5 and 3.0 T: initial observations. Radiology 2001; 221:550–556.